Coresident Sensor Fusion and Compression Using the Wavelet Transform

March 11, 1996

David A. Yocky
Sandia National Laboratories
Albuquerque, NM 87185-0573

ABSTRACT

Imagery from coresident sensor platforms, such as unmanned aerial vehicles, can be combined using multiresolution decomposition of the sensor images by means of the two-dimensional wavelet transform. The wavelet approach uses the combination of spatial/spectral information at multiple scales to create a fused image. This can be done in both an *ad hoc* or model-based approach. We compare results from commercial "fusion" software and the *ad hoc* wavelet approach. Results show the wavelet approach outperforms the commercial algorithms and also supports efficient compression of the fused image.

1. Introduction

The number of commercially available satellite and airborne sensors and the data they provide are continually increasing. Each sensor has its mission and applications. For many applications, the combined information from multiple sensors provides more comprehensive information by collecting at diverse wavelengths, spatial resolutions, and look-angles. Multiple sensor exploitation also means multiple data set manipulation with some sets being quite large. Potentially massive data sets demand exploration of integration of the relevant information into a concise, manageable data set.

This paper addresses "fusing" information by exploring a wavelet technique of combining sensor information via image merging. We briefly compare the performance of an *ad hoc* wavelet technique to two commercially available merging techniques. We then discuss why the *ad hoc* technique is well suited for coresident image fusion and compression.

This work was supported by the United States Department of Energy under Contract DE-AC04-94AL85000.

2. Image Merging

Image merging refers to image processing techniques that combine image sets from two or more sensors to generate an enhanced final image. Past image merger research explored combining spectral information from a low spatial resolution multispectral sensor with high spatial resolution imagery.[1-23] The resultant merged image is useful in enhancing image mensuration as well as localizing phenomena. Spatial enhancement while preserving spectral fidelity is the goal of such mergers. If this goal is achieved, the end product provides enhanced data for spectral/spatial classification and automatic target recognition (ATR) algorithms.

Image merging should be of interest to defense and intelligence-gathering entities. With the advent of multisensor platforms, such as an unmanned aerial vehicle (UAV), that have access to denied territory, image fusion of coresident sensors before exploitation would give enhanced imagery. Image fusion would also reduce the communication or storage requirements. The ideal platform would include coresident sensors that are coregistered (i.e., share the same collection optics) so that registration would not be an additional computational step. The Tier II Plus UAV would be a likely candidate.[24]

Recently, we explored image merging using the two-dimensional wavelet transform, which is well suited for coresident, coregistered sensor fusion.[22,23] The wavelet merger is accomplished by decomposing separate sensor images into decreasing resolution components. Each decomposition forms a pyramid. From these pyramids, the wavelet building blocks can be reassembled into one pyramid using many different approaches. The decomposition can then be reversed to give a fused image.

Our goal in using the multiresolution wavelet decomposition (MWD) image merger was to combine spectral and spatial information in an efficient manner without significant trade-offs in spectral or spatial fidelity. The measure of performance was the amount of spectral degradation created by adding spatial information. The performance of the MWD merger was compared to two commercially available techniques: the intensity modulation (IM) and the intensity-hue-saturation (IHS) mergers.

3. Merging Techniques

In the following, we present the merging techniques used for comparison. The techniques assume there are two images, one "multispectral" image and one "panchromatic" image. The color multispectral image channels are assigned the color gun designations red, green, and blue (RGB).

3.1 Intensity Modulation Merger

The IM merger method normalizes each color band to unity and multiplies each pixel value by the corresponding panchromatic pixel value to produce the merged image. Cliche et al.[5] used an IM method in combining simulated multispectral and panchromatic data. Others have used IM for combining synthetic aperture radar and multispectral imagery.[25,26]

3.2 Intensity-Hue-Saturation Merger

The IHS merger transforms the RGB multispectral channels into IHS components. Intensity is the total color brightness. Hue refers to the dominant wavelength contributing to a color. Saturation specifies the vividness of the color with respect to gray. To create the merger, the intensity component is replaced by

the high spatial resolution panchromatic data. The transform is reversed to create an RGB image with merged panchromatic information. RGB to IHS algorithms can be found in Haydn et al.,[8] Shettigara,[18] and Smith.[27]

3.3 Multiresolution Wavelet Decomposition Merger

Multiresolution decomposition[28-30] provides a pyramid hierarchy for image manipulation and analysis at different resolution levels. The wavelet transform can also provide this type of decomposition along with good localization in both spatial and Fourier domains.[31-34]

The orthogonal wavelet decomposition of a signal produces a reduced resolution signal approximation and a detail signal. Lower resolution signal approximations are derived by applying a low-pass filter and subsampling the output by two. The detail signals are produced by applying the quadrature mirror high-pass filter[31] and subsampling by two. Perfect reconstruction of the original signal requires the filter pair to have regularity constraints.[33]

The discrete two-dimensional wavelet transform (2DWT) produces one image approximation and three detail images. The three detail images are a set of independent, spatially-oriented frequency channels that detail vertical high frequencies, horizontal high frequencies, and cross-directional high frequencies.[31]

3.4 *Ad Hoc* Approach

The MWD merging of two data sets uses identically sized registered images where resolution differences are usually addressed by resampling the low-resolution image to the high-resolution image spacing. The wavelet basis and final decomposition resolution is chosen, and the MWD is performed on both images. The generic structure is shown in Figure 1. The simplest merger approach takes the desired sensor image approximation from its decomposition pyramid replacing the approximation image in the other sensor's decomposition pyramid. For example, the low-resolution, multispectral approximation is substituted for the panchromatic approximation. The inverse MWD is then performed on the combined image. Simple *ad hoc* variations using both decomposition pyramids in reconstruction have also been explored.[23] We developed the MWD using the KHOROS Cantata programming environment.

3.5 Other Approaches

Others have also developed wavelet image fusion approaches. Each approach is similar in decomposition, but the combination or interpolation of wavelet coefficients is different and more computer intensive. The model-based approach takes the decomposed resolution levels of two spatial resolution sensors and constructs a predictive model using coexisting resolution information.[16] For the low-resolution sensor, wavelet coefficients are interpolated using the model, creating the missing high-resolution levels. The reconstructed low-resolution pyramid with the interpolated levels produces a final enhanced image with spatial resolution close to the high-resolution sensor. Figure 2 shows this approach.

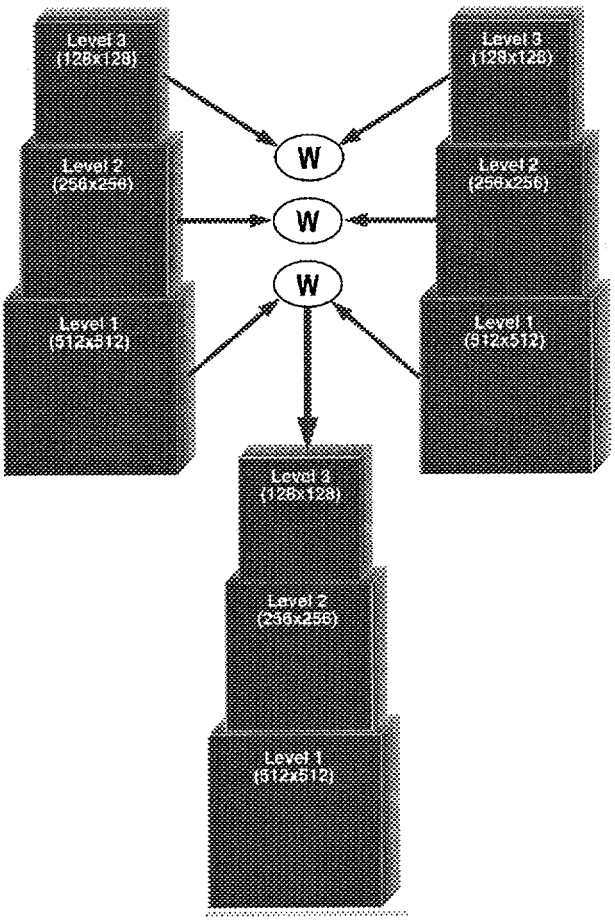

Figure 1. Ad-hoc wavelet image merger approach.

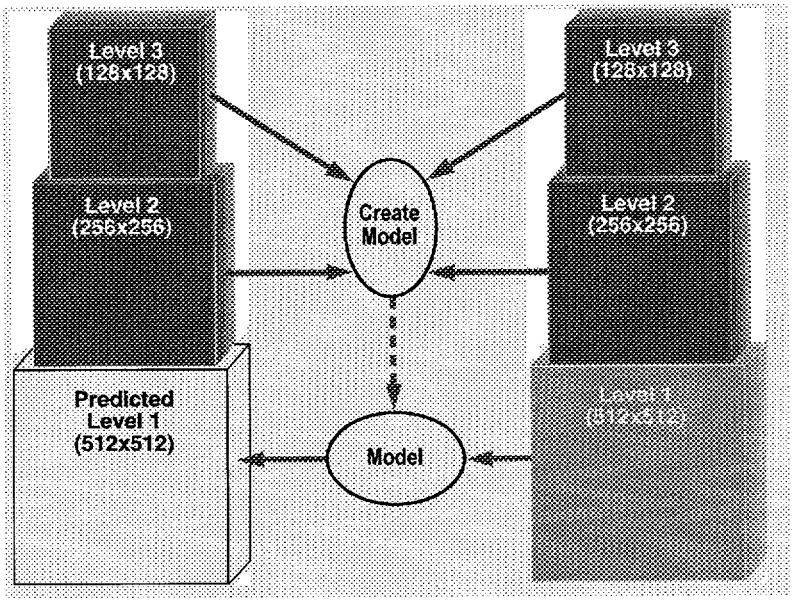

Figure 2. Model-based wavelet image merger approach.

Another wavelet fusion technique uses the contrast sensitivity function of the human eye as a basis for reconstruction.[21] The disparate spatial information from different wavelengths is combined into a final aesthetically pleasing spatial image. Spectral fidelity is not a goal of this approach.

Although there has not been a comparison of wavelet techniques, we considered only the model-based or *ad hoc* approaches because of our spectral fidelity goal. From those approaches, we chose the *ad hoc* MWD because of its simplicity, although more complex approaches may be more applicable for some data sets.

3.6 Computation Time

The computational time of performing such mergers on a remote sensing platform should be minimized. For N data points, IM, IHS, and MWD algorithms are $O(N)$. In comparison, the order of complexity of the fast Fourier transform (FFT) is $O(N \log_2 N)$.

4. Merger Comparison

In comparing the three merging techniques, we used test images that were manipulated and compared to the original, which was used as "ground truth." We also looked at the effects of input misregistration on the final merged images.

The image mergers were conducted according to the techniques described above. The MWD merger used simple, orthonormal bases called Daubechies wavelets[33] selected for their mathematical properties to present the MWD concept. The *ad hoc* MWD used the Daubechies six-coefficient wavelet, and the pyramids were always taken to the 1/8-resolution level. The results are denoted as MWD.

4.1 Statistical Metrics

The spectral and spatial quality is quantified by the difference in means ($\Delta\mu$), the difference in standard deviations ($\Delta\sigma$), the difference in entropy (ΔH), and the area affected. The mean and standard deviation are well-known statistics. Entropy is from Shannon's information theory[35] and is defined as

$$H = -\sum_{i=0}^{N-1} P_i \log (P_i)$$

where P_i is the probability of gray level i for an image having N gray levels.

In combining the panchromatic and the multispectral data, we strive for reconstruction of the original image. A difference in mean would indicate a bias. A difference in standard deviation or a difference in entropy would indicate a change in gray level distribution. The affected area is the percentage of merged image pixels that deviate from the ideal outcome.

4.2 Test Images

We used the color mandrill image found in most image processing libraries as a test image. The

original mandrill image was processed to simulate images sensed by two different sensors. One image simulates a multispectral image created by subsampling and low-pass blurring the original RGB image at 1/4 the spatial resolution of the original image. The pixels were replicated to create a 512 x 512 image. The other image simulates a high-resolution, black and white (panchromatic) image by using the average RGB pixel value for each pixel. Figure 3 shows the original red-band, low-resolution red-band, and panchromatic image. For the registration study, the final low-resolution mandrill image was translated two pixels in both x- and y-directions.

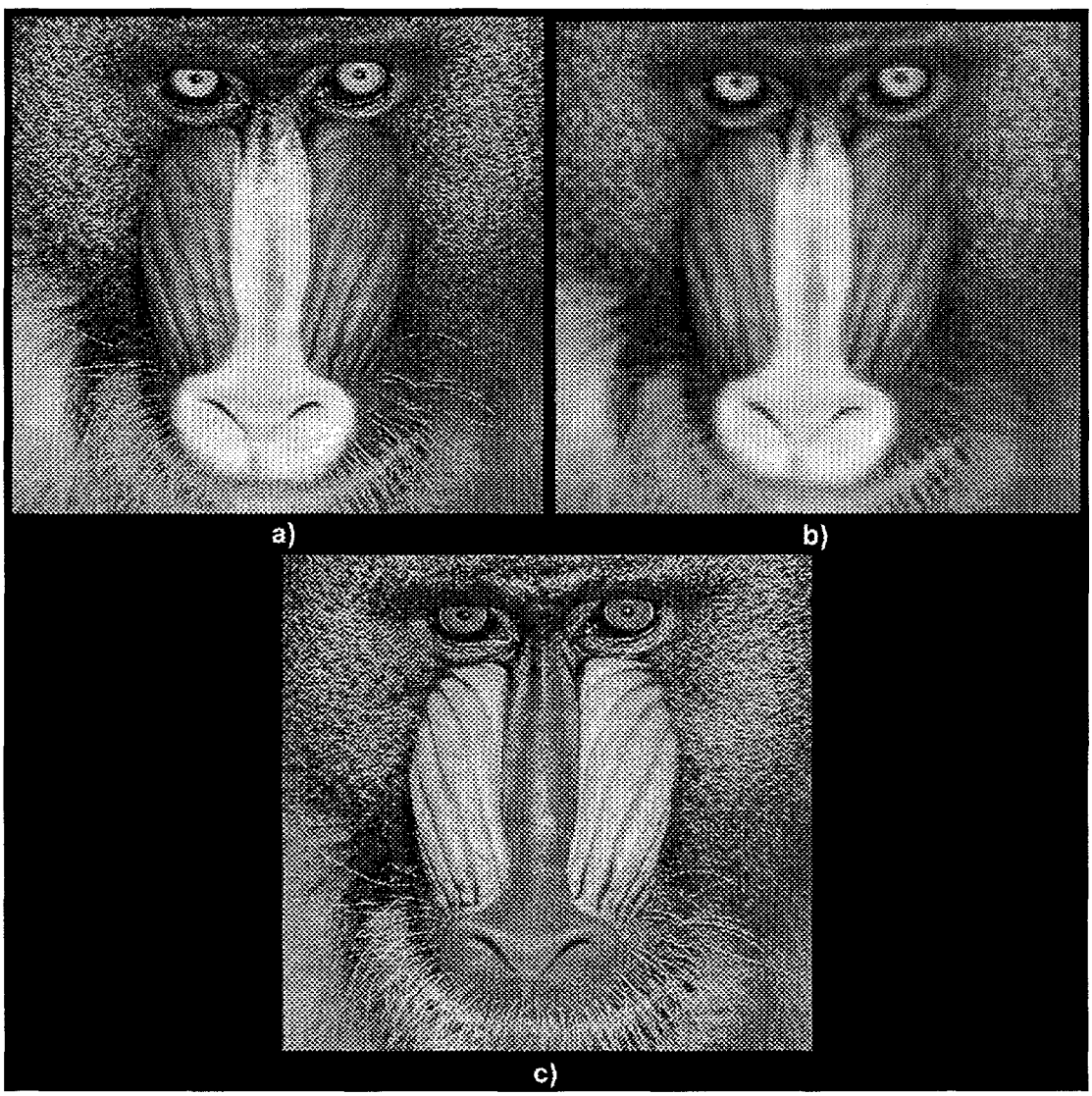

Figure 3. Original mandrill test images--a) original RGB image, b) low-resolution RGB image, c) high-resolution panchromatic image.

4.3 Results

The merged red-band mandrill images are shown in Figure 4. The IM merged image, Figure 4a, is degraded and darker than the original. Sharp spatial features are evident in the merger from the high-contrast edges in the original panchromatic image. Table 1 gives the statistical results. Spectral performance is sacrificed for better spatial performance.

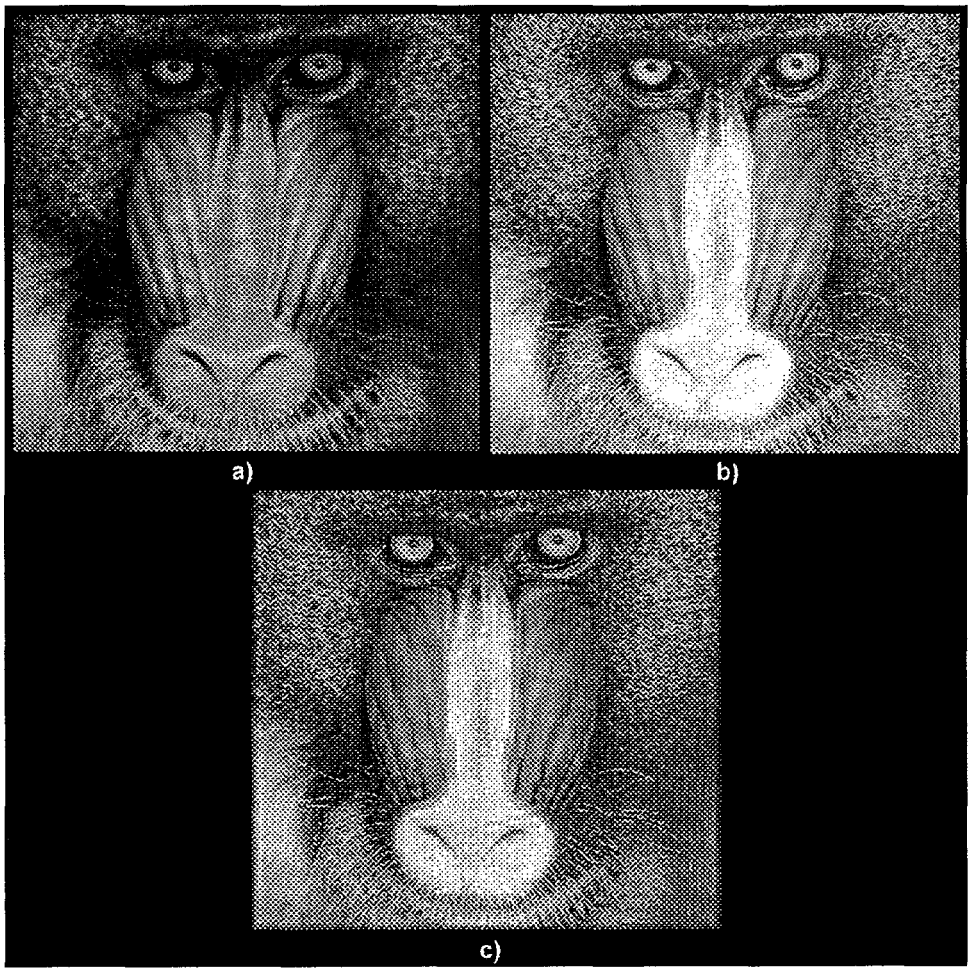

Figure 4. a) Intensity modulation, b) intensity-hue-saturation, and c) multiresolution wavelet decomposition comparison.

Table 1 shows the IHS merger performs consistently across all three bands. However, there is substantial deviation in the mean and standard deviation measures because of large spectral changes. The final image is shown in Figure 4b. The merger suffers from sawtooth artifacts along the mandrill's red nose.

The MWD merged image is shown in Figure 4c. The merged mandrill image has smoothed sawtooth artifacts around the nose and snout. However, the deviations from the mean and standard deviation are almost an order of magnitude better than the IHS in all cases. The affected area is also smaller. The difference in entropy denotes a small increase in gray level uniformity in the final image.

Misregistration does not substantially affect the merging statistics for each merger, as is seen in Table 2. However, Figure 5 shows that the MWD merger suffers from ringing in the mandrill snout due to sensitivity of the MWD to edge location.[36,37]

Table 1: Statistical Comparison between IM, IHS, and MWD Techniques.

Image	$\Delta\mu$	$\Delta\sigma$	ΔH	Affected Area (%)
IM (red)	-52.9442	1.2117	-0.2026	90.38
IM (green)	-30.0387	4.6776	0.1628	90.92
IM (blue)	-12.6655	-7.3736	-0.1129	90.58
IHS (red)	16.1230	4.8712	-0.0935	88.60
IHS (green)	16.8230	5.5263	0.1291	90.26
IHS (blue)	16.7670	4.6216	-0.1086	89.15
MWD (red)	-2.1850	0.8824	0.2238	85.77
MWD (green)	-2.1020	-0.7501	0.1740	79.13
MWD (blue)	-1.6160	-0.9781	0.1454	85.35

Table 2: Statistics for Image Misregistration Case.

Image	$\Delta\mu$	$\Delta\sigma$	ΔH	Affected Area (%)
IM (red)	-40.4147	-8.5443	-0.1048	92.62
IM (green)	-28.5593	4.4104	0.2105	92.45
IM (blue)	-32.9958	-4.3791	-0.2521	92.13
IHS (red)	15.8550	4.8150	-0.1013	90.04
IHS (green)	16.8480	5.0708	0.1231	91.56
IHS (blue)	16.6580	4.2926	-0.1106	90.42
MWD (red)	-2.0950	0.8059	0.2054	88.90
MWD (green)	-1.9610	-0.8446	0.1717	86.83
MWD (blue)	-1.5720	-1.0151	0.1460	89.40

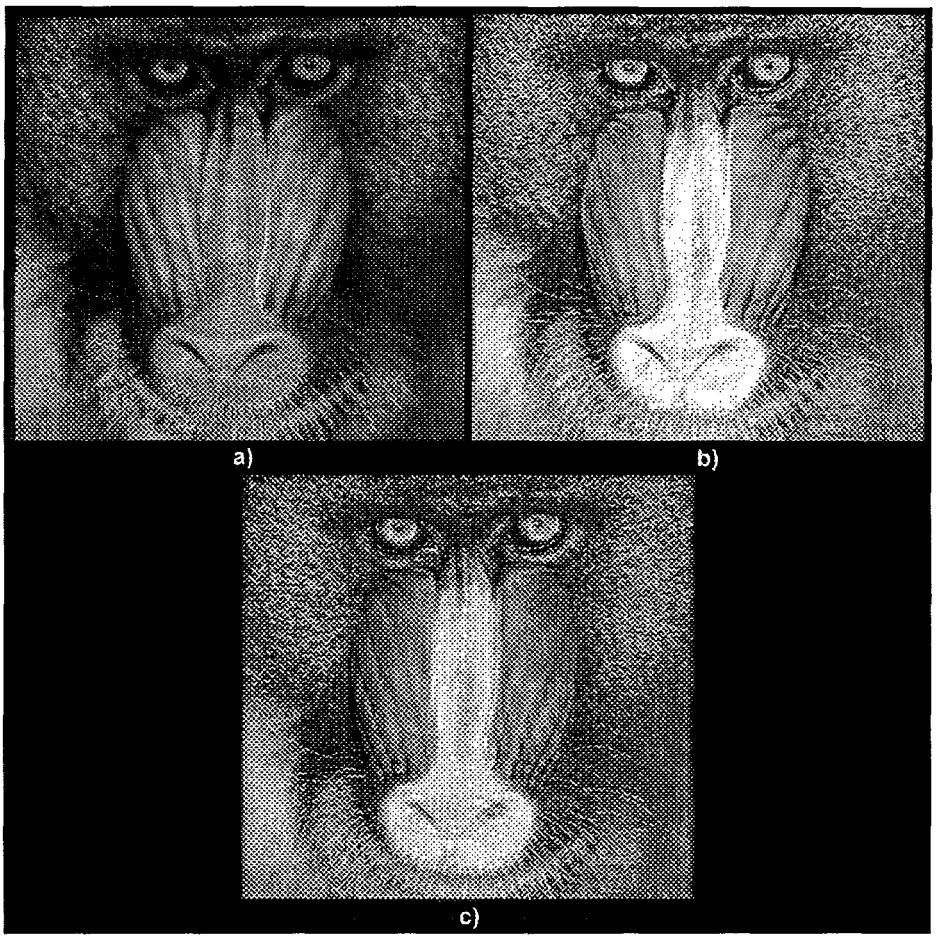

Figure 5. Misregistration effects on--a) intensity modulation, b) intensity-hue-saturation, and c) multiresolutuon wavelet decomposition image merging.

5. Landsat/SPOT merger

Since we did not have UAV or coresident sensor data sets, we merged Landsat Thematic Mapper (TM) and SPOT (Systeme Pour l'Observation de la Terre) panchromatic images as a satellite data example. A Landsat TM image acquired on August 15, 1992, and SPOT panchromatic data acquired on November 7, 1993, over Albuquerque, New Mexico, were used. The original TM green band, SPOT panchromatic, and merged green band are shown in Figure 6. The MWD again outperformed the IHS merger with this type of data.[23]

6. Coresident Fusion and Compression

Dual or multisensor UAVs are definitely candidates for wavelet image fusion. Not only does the wavelet approach outperform some other fusion techniques, it allows for platform-based wavelet bases selection. This flexibility permits sensor or mission specific optimization. Efficient on-board fusion is also possible with the advent of electronic wavelet transform chips. The fused imagery will provide combined information for analysts and enhanced spectral/spatial imagery for automatic target recognition.

The MWD also provides the framework for data compression beyond the actual image fusion. Compression may be critical for coresident multisensor UAV platforms to accomplish their missions in terms of imaging rates, on-board data storage, and data transmission.

Wavelet compression has been developed using orthogonal,[38] biorthogonal,[39] wavelet packets,[40] and zero-crossing and local maxima[41] wavelet methods. Using the decomposed image wavelet coefficients, quantization provides compression. Scalar, vector,[42] and joint space-frequency[43] quantization are examples of lossy wavelet compression schemes. Huffman codes and run-length encoding can provide further compression of the quantized wavelet coefficients. This further compression is lossless.

Some of the wavelet compression approaches have advantages over Joint Photographic Experts Group (JPEG) and Motion Picture Experts Group (MPEG) techniques at high compression ratios (greater than 10:1),[44] and since JPEG and MPEG are based on Fourier techniques, the wavelet approach can be computationally faster. The wavelet transform also allows for progressive transmission, as well as compression of background and targets at different rates.

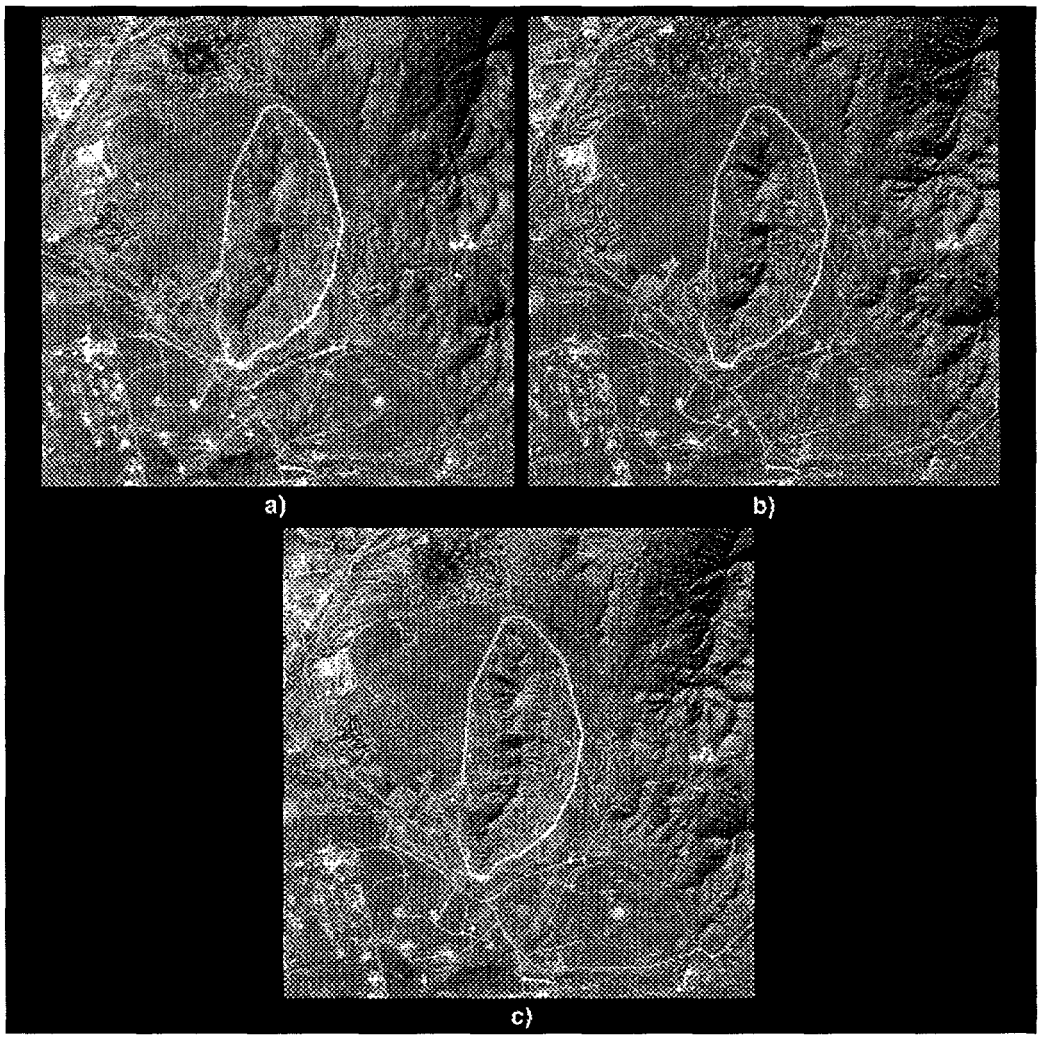

Figure 6. a) Landsat TM band 2, b) SPOT panchromatic, c) wavelet image merger of a) and b).

7. Conclusion

Fusion and compression create a strong foundation for using the wavelet merging approach aboard coresident/coregistered UAV or other multisensor platforms. We found that the MWD image merger outperformed the IM and IHS merging algorithms. With the added luxury of a compression framework, the wavelet image merger would provide enhanced spatial/spectral information for automatic target recognition or image analysts.

8. References

1. W. J. Carper, T. M. Lillesand, and R. W. Kiefer, "The use of the intensity-hue-saturation transformations for merging SPOT panchromatic and multispectral image data," *Photogrammetric Eng. Remote Sensing* **56**(4) pp. 459-467 (1990).

2. P. S. Chavez, Jr., S. C. Guptill, and J. Bowell, "Image processing techniques for thematic mapper data," *Proc. of the 50th Annual ASP-ACSM Symp., Am. Soc. of Photogrammetry*, Washington, D.C., pp. 728-743 (1984).

3. P. S. Chavez, Jr., "Digital merging of Landsat-TM and digitized NHAP data for 1:24,000-scale image mapping," *Photogrammetric Eng. Remote Sensing* **52**(10) pp. 140-146 (1986).

4. P. S. Chavez, Jr., S.C. Sides, and J. A. Anderson, "Comparison of three different methods to merge multiresolution and multispectral data: Landsat TM and SPOT panchromatic, *Photogrammetric Eng. Remote Sensing* **57**(3), pp. 295-303 (1991).

5. G. Cliche, F. Bonn, and P. Teillet, "Integration of the SPOT panchromatic channel into its multispectral mode for image sharpness enhancement," *Photogrammetric Eng. Remote Sensing* **51**(3), pp. 311-316 (1985).

6. D. P. Filiberti, S. E. Marsh, and R. A. Schowengerdt, "Synthesis of imagery with high spatial and spectral resolution from multiple image sources," *Opt. Eng.* **33**(8), pp. 2520-2528 (1994).

7. B. Garguet-Dupont, J. Girel, G. Pautou, "Analyse spatiale d'une zone alluviale pare une nouvelle methode de fusion d'images SPOT multispectrales (XS) et SPOT panchromatique (P)," *C. R. Acad. Sci. Paris* **317**, pp. 194-201 (1994).

8. R. Haydn, G.W. Dalke, J. Henkel, and J. E. Bare, "Application of the IHS color transform to the processing of multisensor data and image enhancement," *Proc. of the International Symp. on Remote Sensing of Arid and Semi-Arid Lands*, Cairo, Egypt, pp. 599-616 (1982).

9. M. Inamura, "Spatial resolution improvement of a low spatial resolution image using spatial component extracted from high spatial resolution images," *IGARSS '93*, pp. 2105-2107 (1993).

10. A. E. Iverson, and J. R. Lersch, "Adaptive image sharpening using multiresolution representations," *Proc. of the SPIE on Algorithms for Multispectral and Hyperspectral Imagery* **2231**, pp. 72-83 (1994).

11. D. Izraelevitz, "Model-based multispectral sharpening," *Proc. of the SPIE on Algorithms for Multispectral and Hyperspectral Imagery* **2231**, pp. 60 - 71 (1994).

12. S. M. Moran, "A window-based technique for combining Landsat Thematic Mapper thermal data with higher-resolution multispectral data over agricultural lands," *Photogrammetric Eng. Remote Sensing* **56**(3), pp. 337-342 (1990).

13. C. K. Munechika, J. S. Warnick, C. Salvaggio, and J. R. Schott, "Resolution enhancement of multispectral image data to improve classification accuracy," *Photogrammetric Eng. Remote Sensing* **59**(1), pp. 67-72 (1993).

14. D. Pradines, "Improving SPOT images size and multispectral resolution," *Proc. of the SPIE on Earth Remote Sensing Using the Landsat Thematic Mapper and SPOT Systems* **660**, pp. 98-102 (1986).

15. J. C. Price, "Combining panchromatic and multispectral imagery from dual resolution satellite instruments," *Remote Sensing Environ.* **21**(2), pp. 119-128 (1987).

16. T. Ranchin, L. Wald, and M. Mangolini, "Efficient data fusion using the wavelet transform: the case of SPOT satellite images," *Proc. of the SPIE Conference on Math. Imaging: Wavelet Applications in Signal and Image Processing* **2034**, pp. 171-178 (1993).

17. R. A. Schowengerdt, "Reconstruction of multispatial, multispectral image data using spatial frequency content," *Photogrammetric Eng. Remote Sensing* **46**(10), pp. 1325-1334 (1980).

18. V. K. Shettigara, "A generalized component substitution technique for spatial enhancement of multispectral images using a higher resolution data set," *Photogrammetric Eng. Remote Sensing* **58**(5), pp. 561-567 (1992).

19. V. T. Tom, M. J. Carlotto, and D. K. Scholten, "Spatial sharpening of thematic mapper data using a multiband approach," *Opt. Eng.* **24**(6), pp. 1026-1029 (1985).

20. E. Waltz, "The principles and practice of image and spatial data fusion," in *Proc. of the 8th National Symp. on Sensor Fusion, Vol. I*, pp. 257-278 (1994).

21. T. A. Wilson, S. K. Rogers, and L. R. Myers, "Perceptual-based hyperspectral image fusion using multiresolution analysis," *Opt. Eng.* **34**(11), pp. 3154-3164 (1995).

22. D. A. Yocky, "Image merging and data fusion by means of the discrete two-dimensional wavelet transform," *J. Opt. Soc. Am. A.* **12**(9) pp. 1834-1841 (1995).

23. D. A. Yocky, "Multiresolution wavelet decomposition merger of Landsat Thematic Mapper and SPOT panchromatic data," *Photogrammetric Eng. Remote Sensing*, (accepted paper).

24. C. F. Lam, and J. N. Entzminger, "The high altitude endurance unmanned aerial vehicle program," in *Proc. of the 8th National Symp. on Sensor Fusion, Vol. I*, pp. 189-214 (1994).

25. M. I. Daily, T. Farr, and G. Elachi, "Geologic interpretation from composited radar and Landsat imagery," *Photogrammetric Eng. Remote Sensing* **45**(8), pp. 1109-1116 (1979).

26. F. H. Wong and R. Orth, "Registration of Seasat/Landsat composite images to UTM coordinates," *Proc. of the 6th Canadian Symp. on Remote Sensing*, Halifax, Nova Scotia, pp. 161-165 (1980).

27. A. R. Smith, "Color gamut transform pairs," *Computer Graphics* **12**(3), pp. 12 -19 (1978).

28. P. J. Burt, "Multiresolution techniques for image representation, analysis, and "smart" transmission," *Proc. of the SPIE Conference on Visual Communication and Image Processing* **1199**, pp. 2-15 (1989).

29. M. D. Levine, *Vision in Man and Machine*, McGraw Hill, San Francisco (1985).

30. H. Wechsler, *Computational Vision*, Academic Press, San Diego (1990).

31. S. G. Mallat, "A theory for multiresolution signal decomposition: the wavelet representation," *IEEE Trans. Pattern Anal. Mach. Intell.*, pp. 674-693 (1989).

32. S. G. Mallat, "Multifrequency channel decompositions of images and wavelet models", *IEEE Trans. Acoust. Speech and Sig. Proc.* **37**(12), pp. 2091-2110 (1989).

33. I. Daubechies, "Orthonormal bases of compactly supported wavelets," *Commun. Pure Appl. Math.* **91**, pp. 909-996 (1988).

34. I. Daubechies, "The wavelet transform, time-frequency localization and signal analysis," *IEEE Trans. Inform. Theory* **36**(5), pp. 961-1005 (1990).

35. C. E. Shannon, "A mathematical theory of communication," *Bell Sys. Tech. J.* **27**, pp. 379-423, 623-656 (1948).

36. G. T. Strang, "Wavelets and dilation equations: A brief introduction," *SIAM Rev.* **31**, pp. 614-627 (1989).

37. J. D. Villasenor, B. Belzer, and J. Liao, "Wavelet filter evaluation for image compression," IEEE Trans. on Image Processing 4(8), pp. 1053-1060 (1995).

38. J. Rosiene and I. Greenshields, "Standard wavelet basis compression of images," *Opt. Eng.* **33**(8), pp. 2572-2578 (1994).

39. M. Antonini, M. Barlaud, P. Mathieu and I. Daubechies, "Image coding using wavelet transform," *IEEE Trans. Image Processing* **1**(2) pp. 205-220 (1992).

40. R. R. Coifman, Y. Meyer, S. R. Quake, and M. V. Wickerhauser, "Signal processing and compression with wavelet packets," *Proc. of the International. Conference on Wavelet Applications*, Toulouse, France, pp.77-93 (1992).

41. J. Fremont and S. Mallat, "Second generation compact image coding with wavelets," in *Wavelets: A Tutorial in Theory and Application*, ed. C. K. Chui, Academic Press, San Diego pp. 655-678 (1992).

42. M. Antonini, M. Barlaud, and P. Mathieu, "Digital image compression using vector quantization and the wavelet transform," *Proc. of the International Conference on Wavelet Applications*, Marseille, France, pp. 160-174 (1989).

43. Z. Xiong, K. Ramchandran, M. T. Orchard, and K. Asai, "Wavelet packets-based image coding using joint space-frequency quantization," *Proc. of IEEE International Conference on Image Processing*, Austin, Texas, pp. 324-328 (1994).

44. T. Hopper and F. Preston, "Compression of grey-scale fingerprint images," *Proc. of IEEE Conference on Data Compression*, Los Alamitos, California, pp. 309-317 (1992).

DISCLAIMER